Effects of ring substituents on electrocatalytic activity of manganese phthalocyanines towards the reduction of molecular oxygen

Nthapo Sehlotho and Tebello Nyokong

Abstract

Reduction of oxygen electrocatalyzed by adsorbed films of manganese phthalocyanine complexes is reported. The complexes studied were: manganese phthalocyanine (MnPc, 1); manganese tetraamino phthalocyanine (MnTAPc, 2); manganese tetrapentoxy pyrrole phthalocyanine (MnTPePyrPc, 3); manganese tetra phenoxy pyrrole phthalocyanine (MnTPPyrPc, 4); manganese tetra mercaptopyrimidine phthalocyanine (MnTMPyPc, 5) and manganese tetra ethoxy thiophene phthalocyanine (MnTETPc, 6). The reaction was conducted in buffer solutions of pH range 1–12. Rotating disk electrode voltammetry revealed two electron reduction in acidic and slightly alkaline media due to the formation of hydrogen peroxide. In highly basic media, water is the major product formed via four electron transfer. The reaction was found to be first order in the diffusing analyte oxygen.

1. Introduction

Oxygen reduction is a very important reaction, both biologically and industrially. It is a cathode reaction in fuel cells, potentially efficient, emission free energy source [1] and [2]. The reaction should occur at a low potential for efficient energy production. It is desirable that the reaction goes to completion and forms water via a four electron transfer mechanism. However, oxygen gets reduced to hydrogen peroxide via a two electron process but the peroxide can still get reduced further via another two electron process to form water.

Platinum electrocatalyses reduction of oxygen to water in fuel cells [1] and [2]. Pt is however an expensive metal hence substitutes have to be found. N_4 metal chelates such as metallophthalocyanines (MPcs) and metalloporphyrins (MPs) have been studied as precious metal fuel cell alternative electrocatalysts [3]. Porphyrins interact with oxygen in nature so oxygen reduction is not alien to them [4]. However, they are less thermally and chemically stable compared to MPc complexes. The catalytic performance of MPc complexes depends on the central metal, ligands and support [5], [6], [7] and [8]. Their activity towards oxygen reduction is better with dimeric species than their monomeric counterparts. This was observed with *μ*-oxo-bridged dimer of an iron(III) phthalocyanine complex [9]. The geometry was reported [9] to be cofacial on electrodes facilitating coordination and splitting of oxygen. Generally, MPcs are efficient in alkaline solutions even though this medium poses difficulty of electrolyte decarbonation [10] and [11]. The setbacks of MPc complexes as electrocatalysts for reduction of oxygen include promotion of two electron (instead of four) transfer process yielding hydrogen peroxide [1] and [2]. However, thicker films obtained by polymerization were reported to promote four electron transfer process and are also stable [7].

In this study, a series of manganese phthalocyanine complexes tetra-substituted with different peripheral ligands (Fig. 1) have been used as electrocatalysts for oxygen reduction. The complexes are: manganese phthalocyanine (MnPc, 1); manganese tetraamino phthalocyanine (MnTAPc, 2); manganese tetrapentoxy pyrrole phthalocyanine (MnTPePyrPc, 3); manganese tetra phenoxy pyrrole phthalocyanine (MnTPPyrPc, 4); manganese tetra mercaptopyrimidine phthalocyanine (MnTMPyPc, 5) and manganese tetra ethoxy thiophene phthalocyanine (MnTETPc, 6). Glassy carbon electrode is modified by adsorption and the catalytic reduction is carried out in a pH range of 1–12. Effect of ring substituents on electrocatalytic activity is investigated.

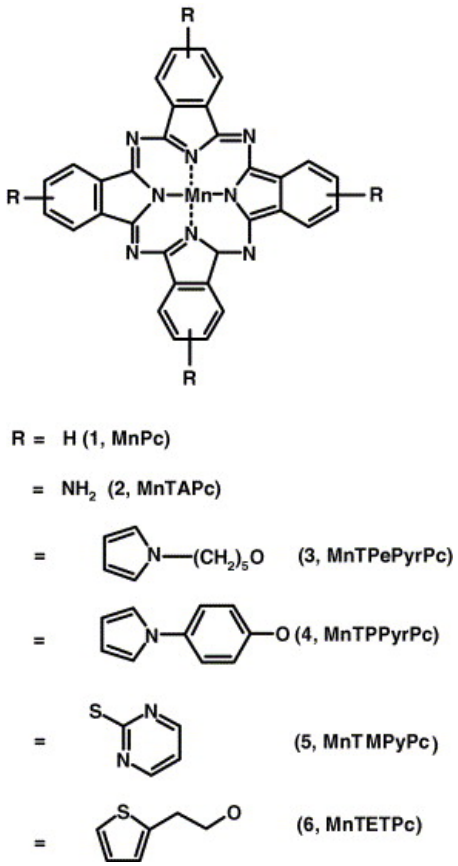

Fig. 1. Molecular structures of manganese phthalocyanine complexes: Manganese phthalocyanine (MnPc, 1); manganese tetraamino phthalocyanine (MnTAPc, 2); manganese tetrapentoxy pyrrole phthalocyanine (MnTPePyrPc, 3); manganese tetra phenoxy pyrrole phthalocyanine (MnTPPyrPc, 4); manganese tetra mercapto-pyrimidine phthalocyanine (MnTMPyPc, 5) and manganese tetra ethoxy thiophene phthalocyanine (MnTETPc, 6).

2. Experimental

2.1. Materials and synthesis

pH 4 and 7 buffer tablets, H_2SO_4, NaOH, ethanol, hydrogen peroxide (H_2O_2), dimethylformamide (DMF), dichloromethane (DCM), methanol, glacial acetic acid, manganese chloride, lithium, hydrochloric acid, sodium chloride, calcium chloride, potassium carbonate, sodium sulphate, and dimethylsulfoxide (DMSO) were purchased from SAARCHEM while $NaBH_4$ was purchased from UNILAB. 5-Amino pentanol, dimethoxytetrahydrofuran, tetrabutylammonium tetrafluoroborate ($TBABF_4$) and 1-pentanol were from Aldrich. Solvents were distilled before use while other reagents were used as received. Buffer solutions in the range 1–12 were made from pH 4 and pH 7 solutions by adjusting the pH with addition of acid (0.5 M H_2SO_4) or alkali (0.5 M NaOH) as required.

Manganese phthalocyanine (MnPc, 1) was purchased from EASTMAN. The syntheses of the following complexes (Fig. 1) have been reported by our group before: manganese tetraamino phthalocyanine (MnTAPc, 2) [12]; manganese tetra phenoxy pyrrole phthalocyanine (MnTPPyrPc, 4) [13]; manganese tetra mercaptopyrimidine phthalocyanine (MnTMPyPc, 5) [14] and manganese tetra ethoxy thiophene phthalocyanine (MnTETPc, 6) [15]. Manganese tetrapentoxy pyrrole phthalocyanine (MnTPePyrPc, 3) was synthesized by adopting a procedure reported before [16] and [17] for the synthesis of tetra propoxy pyrrole substituted metal phthalocyanines. Details are provided as supplementary materials.

2.2. Electrochemical methods

Electrochemical experiment set-ups consisted of a three electrode system consisting of glassy carbon electrode (0.071 cm^2) as a working electrode, platinum wire as a counter while Ag|AgCl was a pseudo-reference electrode. Cyclic voltammograms (CV) were recorded using BioAnalytical Systems (BAS) 100 B/W Electrochemical Workstation. The glassy carbon electrode was polished on alumina (<10 μM) slurries on a BAS feltpad. This was followed by rinsing with Millipore water and then ethanol. The electrode was modified by placing a drop of 1 mM MnPc solution in DMF for three minutes to allow adsorption, after which the electrode was rinsed with DMF, to remove residual solution, followed by ethanol before use. pH values were measured using a pH meter (WTW, Germany). Characterization of the adsorbed MPc films was done in buffer solutions deaerated with nitrogen. Oxygen gas was bubbled for 10 min to attain saturation for oxygen reduction experiments. Oxygen reduction studies using CV and rotating disc electrode (RDE) voltammetry were then conducted. UV/Vis spectra were recorded with Cary 500 UV/Vis Spectrophotometer.

3. Results and discussion

3.1. Characterization of adsorbed MPc films

For characterization purposes, cyclic voltammograms (CVs) of adsorbed MPc complexes were run in nitrogen-purged buffer solutions in the pH range 1–12. Only studies in pH 5 and 12 are shown in Fig. 2 using complex 4 as an example. The adsorbed MnPc derivatives (curve i in Fig. 2a), exhibited $Mn^{III/II}$ processes (labeled I) at; −0.35, −0.25, −0.12, −0.29, −0.26 V and −0.41 for complexes 1–6, respectively, in comparison with literature [12], [13], [14] and [15]. The second peak labeled II is associated with ring based reduction and the formation of $Mn^{II}Pc^{-2}/Mn^{II}Pc^{-3}$. Peak potentials for the $Mn^{III/II}$ couple shifted to the negative values with increase in pH, Fig. 3, and a linear behaviour was observed between pH 1 and 6. An average slope of ≈−0.06 V/pH was observed indicating a transfer of one electron per proton.

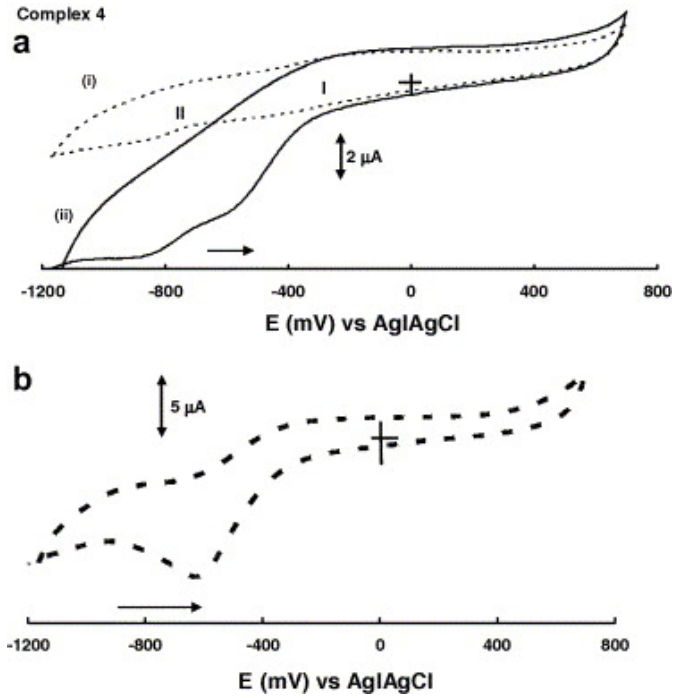

Fig. 2. Cyclic voltammograms of 4. (a) pH 5 buffer: (i) nitrogen-purged and (ii) oxygen saturated. (b) pH 12 buffer in oxygen saturated solution. Scan rate = 50 mV/s.

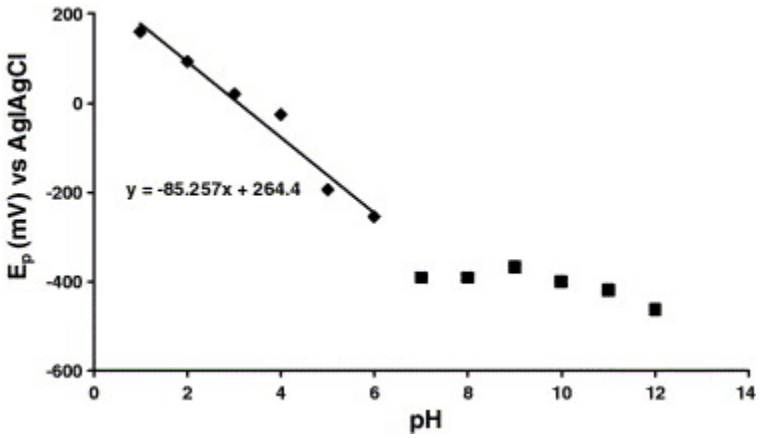

Fig. 3. Pourbaix diagram (Ep versus pH) of $Mn^{III/II}$ couple of complex 3.

Surface coverage was probed by recording the CVs of the complexes at different scan rates (figure not shown) based on Eq. (1) [18]:

$$I_p = n^2F^2\Gamma_{MPc}Av/4RT \quad (1)$$

where n is number of electrons transferred, F is Faraday's constant, A is electrode area, R is the gas constant, T is the temperature and Γ_{MPc} is surface coverage. For all complexes, surface coverage was calculated (from the plots of I_p versus v) to be in the 10^{-10} range indicating monolayer thickness. Linearity of these plots indicated surface confined adsorbed species [19], confirming adsorption of MPc films.

3.2. Oxygen reduction

On MPc modified electrodes, oxygen first gets reduced to hydrogen peroxide, followed by reduction of the latter to water [20], each step requiring two electrons. In acid and slightly alkaline media, the CV for oxygen reduction on MPc modified electrodes shows two reduction peaks due to oxygen reduction to hydrogen peroxide and subsequent hydrogen peroxide reduction to water [20]. In highly alkaline solutions, the reaction goes to completion with only one peak observed due to four electron reduction of oxygen to water [20]. In this study, a similar trend in activity was observed.

Fig. 2a (curve ii, using complex 4 as an example) shows enhancement of currents of the MnPc complexes in the presence of oxygen confirming catalytic reduction of oxygen. Table 1 lists the potentials for oxygen reduction at pH 5 and 12. Two peaks are observed for all complexes at pH 5 (except 2) due to the formation of hydrogen peroxide and water. The presence of the two peaks in the range for $Mn^{III}Pc^{-2}/Mn^{II}Pc^{-2}$ and the ring process $Mn^{II}Pc^{-2}/Mn^{II}Pc^{-3}$ confirms that both of these processes catalyse the oxygen reduction, as has been reported before [20]. However, in highly alkaline solutions (pH 9–12), there is only one peak for most complexes (Fig. 2b), due to reduction of oxygen to water. Extra peaks were however observed at high negative potentials for complexes 1 and 5, which could be due to the reduction of the MnPc complex. Based on the ease of the reduction (shifting of potential to less negative values) of oxygen, which reflects the efficiency of these molecules as catalysts for the process, the MnPc complexes may be ranked as follows: 1 ≈ 3 ≈ 5 > 2 > 6 > 4. The ease of reduction of oxygen is not directly related to the redox potential of the $Mn^{III}Pc/Mn^{II}Pc$ couple, which followed this trend: 6 (−0.4 V) > 1 (−0.35 V) > 4 (−0.29 V) > 5 (−0.26 V) > 2 (−0.25) > 3 (−0.12 V). However, Fig. 4 shows some trend when log of current density at peak potential (1st reduction peak) is plotted versus the $Mn^{III}Pc/Mn^{II}Pc$ potential in that complexes 1, 2, 4 and 5 fall within or close to the straight line while complexes 3 and 6 are way off the straight line.

Table 1.

Reduction potentials for oxygen in the presence of MnPc derivatives

Complex	E_p (mV) (Ag|AgCl)	
	pH = 5	pH = 12
MnPc (1)	−494, −824	−463
MnTAPc (2)	−505	−502
MnTPePyPc (3)	−174, −550	−488
MnTPPyPc (4)	−590, −861	−639
MnTMPyrPc (5)	−530, −750	−563
MnTETPc (6)	−613, −861	−616

Scan rate 50 mV/s.

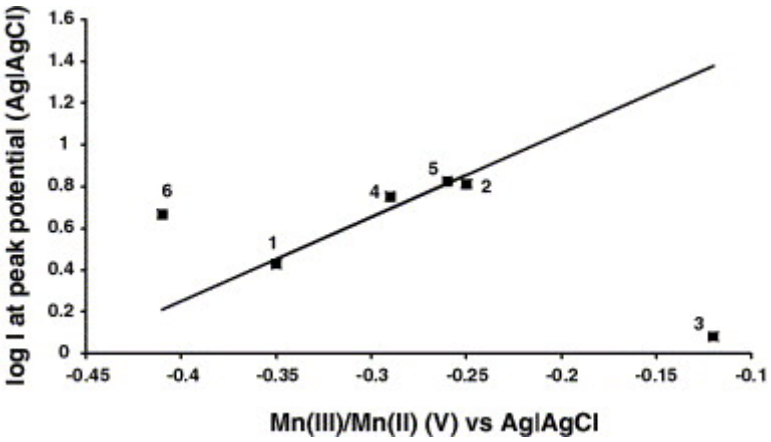

Fig. 4. Plot of log i versus Mn^{III}/Mn^{II} redox potential for oxygen reduction in pH 5 buffer.

The spectra of *μ*-oxo MnPc complexes is well known and is characterized by a high energy absorption at ~630 nm [21]. Complex 3 exists mainly as the *μ*-oxo complex (Fig. 5), while complex 6 also shows considerable amount of the *μ*-oxo species. The rest of the complexes, Fig. 5 (including complex 2 not shown) show insignificant amounts of *μ*-oxo species. Thus both complexes 3 and 6 catalyse the reduction of oxygen using a different species (*μ*-oxo) as opposed to the monomeric MnPc species in the rest of the complexes, hence do not fall within the line in Fig. 4.

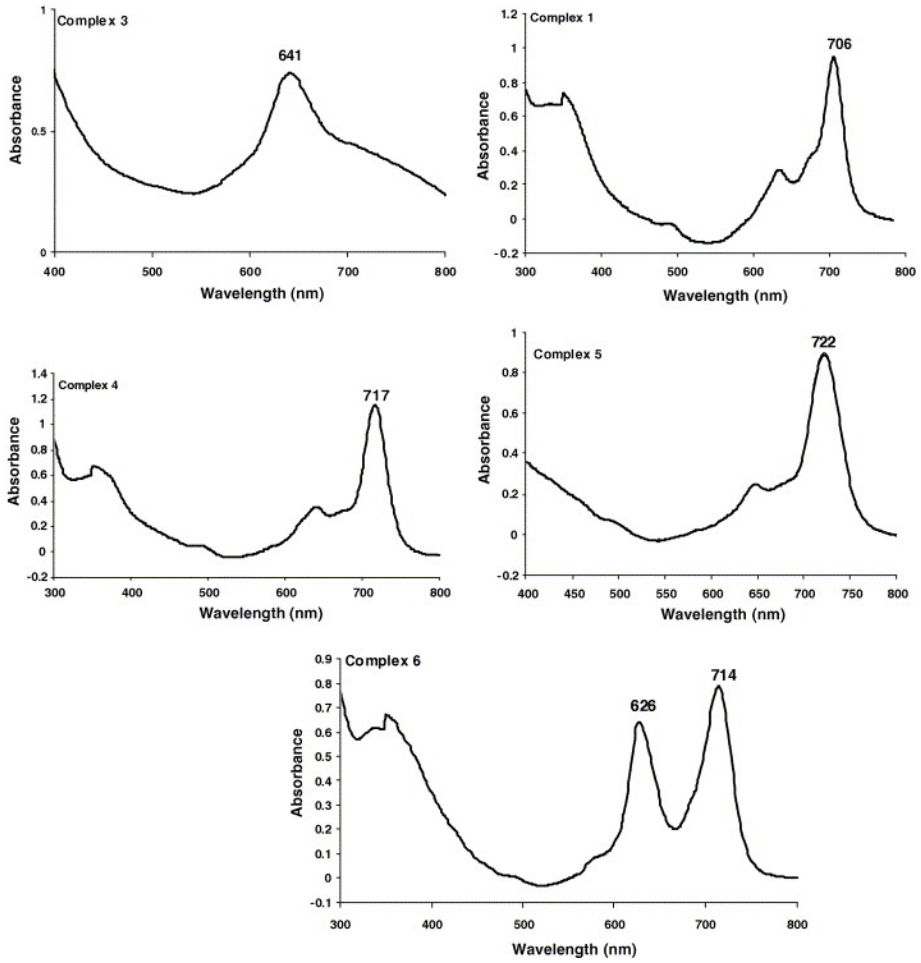

Fig. 5. UV/Visible spectra of complexes 1, and 3–6 in DMF.

Plots of peak current versus square root of scan rate for the reduction of oxygen were linear (figure not shown) for all studied complexes in the pH range 1–12 indicating oxygen reduction to hydrogen peroxide or water is diffusion-controlled.

Rotating disc electrode (RDE) experiments were conducted to further elucidate studied reactions. These experiments were conducted in pH 5, 8 and 12 (Fig. 6 shown for pH 5 and 12) since in these solutions, different mechanisms were highly probable as explained above. Unfortunately only single runs at low rotation speeds were done because the catalyst was lost from the surface. However, runs were done in triplicates and averages are reported. RDE data for the unmodified GCE showed lower currents (Fig. 6b, insert) compared to modified electrodes confirming the catalytic behaviour of the MnPc complexes.

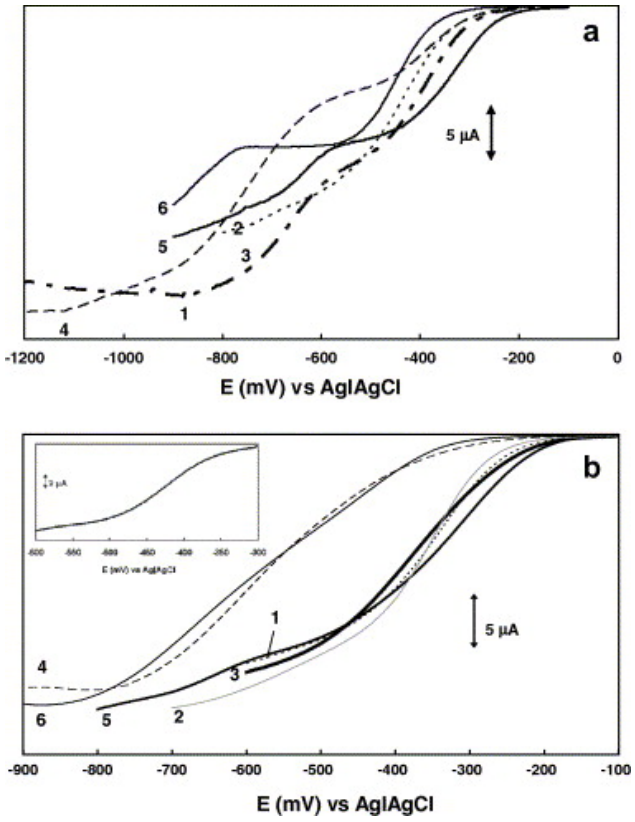

Fig. 6. Rotating disk electrode voltammograms of adsorbed MnPc complexes in pH (a) 5 and (b) 12 oxygen saturated solution at rotation rate of 400 r. p.m. and scan rate of 20 mV/s. Numbers on the CV scans are complex numbers. Insert in (b) is the RDE curve for unmodified GCE in oxygen saturated solution at a rotation rate of 400 r. p.m. and 20 mV/s (pH 12).

The number of electrons transferred during oxygen reduction was calculated from the magnitude of limiting current at 400 rotations per minute (r. p.m.). This was based on Levich equation (2):

$$i_L = 0.62nFAD^{2/3}\omega^{1/2}v^{-1/6}C \qquad (2)$$

where n is number of electrons, F is Faraday's constant, A is electrode area, D is diffusion coefficient, ω is angular rotation rate, v is kinematic viscosity and C is analyte concentration. D, C and v values are 1.67×10^{-5}, 1.3 mM and 9.97×10^{-3} cm^2/s respectively as reported in Refs. [7] and [22]. The total number of electrons transferred was calculated to be 2 at pH 5 and 4 in pHs greater than 5.

Tafel slopes were calculated from the same RDE data. These were obtained from plots of log $|i_K|$ (kinetic current) versus η(reaction overpotential). i_K is current when the system is under complete kinetics, i.e. analyte transport is governed by rotation of the electrode and not diffusion. i_K is equal to $(i_L \times i_m)/(i_L - i_m)$ where i_L is limiting current (plateau in RDE voltammogram) while i_m is measured current and it has to be less than 5% of i_L. Calculated Tafel slopes in pH 5 are shown in Table 2. The values of the Tafel slopes suggest that the first one electron transfer is rate determining. However these values are larger than the expected 120 mV/decade in some cases suggesting binding of the analyte to the catalyst [23], [24] and [25].

Table 2.

Rotating disk electrode parameters of oxygen reduction in pH 5 for complexes 1 to 6

Complex	No. electrons	Tafel slope (mV/decade)	αn_α
MnPc (1)	2.6	−115	0.51
MnTAPc (2)	2.0	−218	0.27
MnTPePyPc (3)	2.2	−177	0.33
MnTPPyPc (4)	2.8	−129	0.46
MnTMPyrPc (5)	2.1	−148	0.40
MnTETPc (6)	1.8	−130	0.45

Electron transfer coefficients (α) were calculated from Tafel slopes using the relationship, Eq. (3) [7]:

$$b = 2.3RT/\alpha n_\alpha F \quad (3)$$

for an irreversible process where n_α is number of electrons involved in the rate determining step. The calculated values of αn_α in pH 5 are shown in Table 2. The values indicate that the mechanism of oxygen reduction by MnPc proceeds through a one-electron rate determining step, with α of approximately 0.5. The αn_α values were not dependant on pH in this work, in contrast to a literature report [7].

The reaction order was determined using Eq. (4) [23]:

$$\log I = \log i_K + m \log\{1 - (i/i_L)\} \quad (4)$$

where m is order and the other parameters have their usual meaning. The reaction order was found to be one for all complexes in the studied pH range. Rate constants can be determined using relationships; $i_K = nFCkA$ where k is electron transfer constant using RDE data [26], and the other constants have their usual meaning. k was found to be in the 10^{-5} range for all complexes in the pH range studied indicating the reaction kinetics are slow.

3.3. Mechanism of oxygen reduction

The interaction between oxygen and MnPc complexes is more prominent compared to interaction of oxygen with MPc containing transition metals such as Fe and Co because Mn has lower energy d orbitals. Energy gap between participating MOs (molecular orbitals) of oxygen and MnPc is described in terms of hardness [26], [27] and [28]. The larger the gap, the higher the hardness and the more stable the system is, hence low reactivity.

Substituents on the MPc have an effect on the MO energy levels. Electron-withdrawing groups lower the energy of the MO of MPc, while their electron-donating counterparts increase it [26]. Lowering of energy levels of MO of MPc minimizes the gap between MPc-MO and that of oxygen. The system becomes soft, the interaction is enhanced and thus reactivity increases. It is therefore theoretically expected that electron-withdrawing ligands will increase catalytic activity of MnPcs towards oxygen reduction. Electron-donating substituents are expected to have an opposite effect. Log k (k = rate constant) of oxygen reduction catalyzed by CoPcs with electron-donating substituents was found to decrease when plotted against sum of Hammett parameters of the substituents [28]. For the MnPc complexes in this work, the ease of reduction of oxygen following the order: 1 ≈ 3 ≈ 5 > 2 > 6 > 4, shows that the unsubstituted complex 1, is a better catalyst than for example 2 (which contains electron- donating substituents) in agreement with literature.

It has been reported that when MnPcs interact with oxygen, either the superoxide or the oxo-bridged dimer are formed [29], [30], [31] and [32]. This has been confirmed with UV/Vis spectroscopy [30] and [31]. Furthermore, it has been reported that oxygen adsorption on the electrode can involve electron transfer leading to its activation as follows:

$S + O_2 = S - O_2^-$ where S is the surface. It can also occur without electron transfer as;

$S + O_2 = S - O_2$, the former has been proven spectroscopically [33].

In this study, formation of adducts upon interaction of MnPc complexes with oxygen was probed using solution UV/Vis spectroscopy, Fig. 7 (for complexes 1 and 3). In all complexes (except 3), the starting species is mainly the $Mn^{III}Pc$ as evidence by the red shifted *Q* band with $\lambda > 700$ nm. Oxygen was bubbled to MnPc solutions in the 3+ state and no significant spectral changes were observed for all complexes. The complexes were then reduced using sodium borohydride and oxygen bubbled again. After reduction (and before bubbling of oxygen), two peaks are observed for complexes 1, 4, 5 and 6. From the well documented UV/Vis spectra of MnPc complexes [12], [13], [14], [15] and [21], the low energy peak ranging from 674 to 688 nm (following reduction), is assigned to $Mn^{II}Pc$ species for complexes 1, 4, 5 and 6. This peak was however very weak for complex 6. As stated above, the higher energy peak ranging from 615 to 626 nm (for 1, 4, 5 and 6) is assigned to the *μ*-oxo complex. For all complexes (except 2), when oxygen was bubbled to the reduced species, the $Mn^{II}Pc$ peaks generally decreased in intensity, and the peak due to the *μ*-oxo species increased in intensity or remained the same. Thus, the spectral data suggests that formation of MnPc oxo species may be important in the reduction of oxygen.

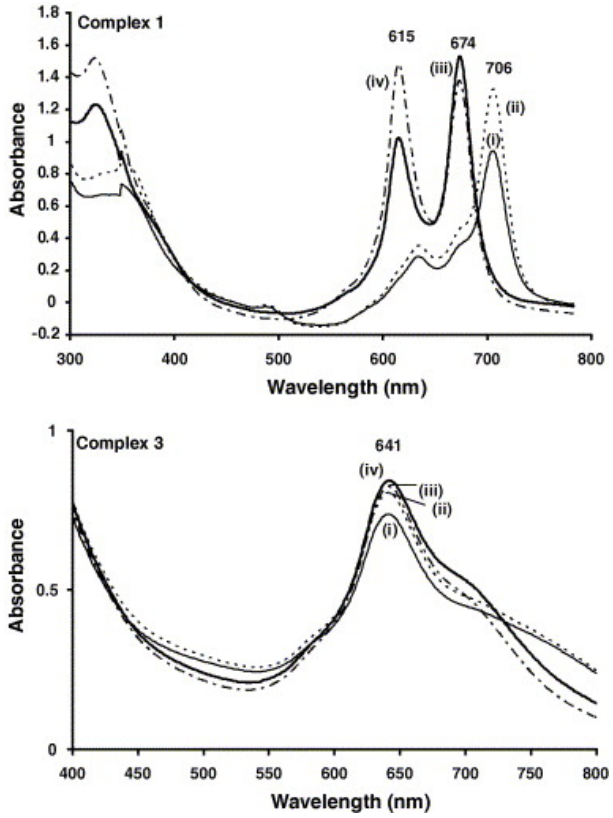

Fig. 7. UV/Visible spectra of complexes 1, and 3 in DMF. (i, —) starting spectrum, (ii, - - -) bubbled oxygen to (i), (iii, ⎯) $NaBH_4$ added to (ii), (iv, - – - –) oxygen bubbled to (iii).

Based on the following observations: (i) in acid and slightly alkaline solutions, two peaks were observed, each due to two electron reduction of oxygen to hydrogen peroxide, and subsequently to water, (ii) Tafel plots proved that the first one electron transfer is rate determining, (iii) protons are involved during the electron transfer and (iii) spectroscopy proved the formation of *μ*-oxo complexes which results from $O_2Mn^{II}Pc$ adduct and that this adduct is best represented as $O_2^- Mn^{III}Pc$[21], the following mechanism (Eqs. (5), (6), (7) and (8)) for oxygen reduction (except for 3) and formation of hydrogen peroxide is proposed:

$$Mn^{III}Pc + e^- \rightarrow Mn^{II}Pc \quad (5)$$

$$Mn^{II}Pc + O_2 \rightarrow (O_2)Mn^{II}Pc \rightarrow (O_2^-)Mn^{III}Pc \quad (6)$$

$$(O_2^-)Mn^{III}Pc + H^+ \rightarrow (O_2H)Mn^{III}Pc \quad (7)$$

$$(O_2H)Mn^{III}Pc + e^- + H^+ \rightarrow Mn^{III}Pc + H_2O_2 \quad (8)$$

4. Conclusion

Manganese complexes of different substituents reduce oxygen to peroxide in acidic or slightly alkaline media and to water in highly alkaline media. The number of electrons transferred is four in alkaline media. Tafel slopes near 120 mV/decade were obtained, implying the transfer of the first electron is rate determining. The reaction order was found to be one. Also the efficiency for oxygen reduction was shown to be related to the ease of the MnPc complexes in forming a *μ*-oxo dimer.

Acknowledgements

This work was supported by Rhodes University and National Research Foundation (NRF, Gun = 2053657) in South Africa. NS thanks NRF and Canon Collins Educational Trust for Southern Africa (CCETSA) for graduate bursary.

References

[1] Phougat, N., Vasudevan, P. Electrocatalytic activity of some metal phthalocyanine compounds for oxygen reduction in phosphoric acid (1997) Journal of Power Sources, 69 (1-2), pp. 161-163

[2] Lalande, G., Faubert, G., Côté, R., Guay, D., Dodelet, J.P., Weng, L.T., Bertrand, P.
Catalytic activity and stability of heat-treated iron phthalocyanines for the electroreduction of oxygen in polymer electrolyte fuel cells (1996) *Journal of Power Sources*, 61 (1-2), pp. 227-237.

[3] Beck, F. (1977) *J. Appl. Electrochem.*, 7, p. 239.

[4] Popovici, S., Leyffer, W., Holze, R. The mechanism of dioxygen reduction at iron meso-tetrakis (Pyridyl) porphyrin: A spectroelectrochemical study (1998) *Journal of Porphyrins and Phthalocyanines*, 2 (3), pp. 249-260.

[5] van Veen, J.A.R., Visser, C. (1979) *Electrochim. Acta*, 24, p. 921

[6] Rodrigues, N.P., Obirai, J., Nyokong, T., Bedioui, F.
Electropolymerized pyrrole-substituted manganese phthalocyanine films for the electroassisted biomimetic catalytic reduction of molecular oxygen. (2005) *Electroanalysis*, 17 (2), pp. 186-190.

[7] Tse, Y.-H., Janda, P., Lam, H., Zhang, J., Pietro, W.J., Lever, A.B.P.
Monomeric and polymeric tetra-aminophthalocyanatocobalt(II) modified electrodes: Electrocatalytic reduction of oxygen. **(**1997) *Journal of Porphyrins and Phthalocyanines*, 1 (1), pp. 3-16.
[8] Zagal, J., Sen, R.K., Yeager, E. (1977) *J. Electroanal. Chem.*, 83, p. 207.

[9] Oyaizu, K., Haryono, A., Natori, J., Tsuchida, E. (1998) J. Chem. Soc. Faraday Trans., 94, p. 3737.

[10] Baranton, S., C. Coutanceau, C. Roux, F. Hahn and J.M. Leger, *J. Electroanal. Chem.* 577 (2005), p. 223.

[11] Coutanceau, C., P. Crouigneau, J.M. Leger and C. Lamy, *J. Electroanal. Chem.* 379 (1994), p. 389.

[12] Obirai, J. and T. Nyokong, *Electrochim. Acta* 49 (2004), p. 1417.

[13] Obirai, J., N.P. Rodrigues, F. Bedioui and T. Nyokong, *J. Porphyrins Phthalocyanines* 7 (2003), p. 508

[14] Obirai, J. and T. Nyokong, *Electrochim. Acta* 50 (2005), p. 3296.

[15] Obirai, J. and T. Nyokong, *Electrochim. Acta* 50 (2005), p. 5427.

[16] Trobach, N., O. Hild, D. Schettwein and D. Wöhrle, *J. Mater. Chem.* 12 (2002), p. 879.

[17] Wöhrle, D., M. Eskes, K. Shigehara and A. Yamada, *Synthesis* (1993), p. 194.

[18] Martel, D., N. Sojic and A. Kuhn, *J. Chem. Educ.* 79 (2002), p. 349.

[19] Mimica, D., F. Bedioui and J.H. Zagal, *Electrochim. Acta* 48 (2002), p. 323.

[20] Ebadi, M., C. Alexiou and A.B.P. Lever, *Can. J. Chem.* 79 (2001), p. 992.

[21] M.J. Stillman and T. Nyokong In: C.C. Leznoff and A.B.P. Lever, Editors, *Phthalocyanines: Properties and Applications* vol. 1, VCH Publishers, New York (1989).

[22] Zhang, J. and F.C. Anson, *J. Electroanal. Chem.* 341 (1992), p. 323.

[23] Zen, J.-M., A. Senthil Kumar and M.-R. Chang, *Electrochim. Acta* 45 (2000), p. 1691.

[24] Lyons, M.E.G., C.A. Fitzgerald and M.R. Smyth, *Analyst* 119 (1994), p. 855

[25] Wermeckers, B. and F. Beck, *Electrochim. Acta* 30 (1985), p. 1491.

[26] Zagal, J.H., M. Gulppi, M. Isaacs, G. Cardenas-Jiron and M.J. Aguirre, *Electrochim. Acta* 44 (1998), p. 1349.

[27] Cardenas-Jiron, G.I., M.A. Gulppi, C.A. Caro, R. del Rio, M. Paez and J.H. Zagal, *Electrochim. Acta* 46 (2001), p. 3227.

[28] Zagal, J.H. and G.I. Cardenas-Jiron, *J. Electroanal. Chem.* 489 (2000), p. 96.

[29] Schlettwein, D., J.P. Meyer and N.I. Jaeger, *J. Porphyrins Phthalocyanines* 4 (2000), p. 23.

[30] Lever, A.B.P., J.P. Wilshire and S.K. Quan, *J. Am. Chem. Soc.* 101 (1979), p. 3668.

[31] Williamson, B.E., T.C. VanCott, M.E. Boyle, G.C. Misener, M.J. Stillman and P.N. Schatz, *J. Am. Chem. Soc.* 114 (1992), p. 2412.

[32] Lever, A.B.P., J.P. Wilshire and S.K. Quan, *Inorg. Chem.* 20 (1981), p. 761

[33] Coutanceau, C., A. Rakotondrainibe, P. Crouigneau, J.M. Leger and C. Lamy, *J. Electroanal. Chem.* 386 (1995), p. 173

Appendix A. Supplementary data

N-pyrrole substituted pentan-1-ol (8, Scheme 1). Compound 8 was synthesized according to the procedure reported for the synthesis of the ethanol analogue [16]. 5-Aminopentanol (50 g, 0.817 mol) was added to 100 mL of glacial acetic acid with continuous stirring. The mixture was cooled in an ice bath containing sodium chloride (NaCl), keeping the temperature below 20 oC since the reaction is exothermic. One portion of 25 g (0.19 mol) of 2,5- dimethoxytetrahydrofuran 7 was then added to the solution while stirring and left to stand for 10 minutes. The acetic acid was distilled off under reduced pressure and the residue was treated with 200 mL of water. The product was extracted five times from water with dichloromethane (DCM). The extracted organic solution was treated, three times, with a saturated aqueous solution of sodium sulfate followed by distilling off DCM. The residue was stirred overnight with a mixture of 30 mL methanol and 30 mL 20% aqueous solution of NaCl. Then the mixture was saturated with NaCl while stirring and left to stand for 30 minutes. The mixture was then transferred into a separating funnel and the organic product was extracted with DCM. Since there were traces of water in the DCM extract the product was dried with calcium chloride.

Finally, DCM was distilled off under reduced pressure. Yield: 30%. IR (KBr) v/cm-1: 3097, 2939, 1655, 1503, 1430, 1280, 1087, 1070, 982, 866, 730. 1HNMR d-DMSO; ä (ppm): 3.6-4.0 (m, 10H, CH2); 6.30(t, 2H, pyrrole); 6.91(t, 2H, pyrrole). 5-(Pyrrol-1-yl)pentoxyphthalonitrile (9, Scheme 1). Compound 9 was synthesized by following literature reports for similar complexes [16]: 5-(pyrrol-1- yl)pentan-1-ol 8 (0.3 g, 1.9 mmol) and 0.27 g (1.56 mmol) of 4-nitrophthalonitrile (synthesized according to reported method [17]) were added to 0.6 g dry K2CO3 in 15 mL dry DMSO. The mixture was stirred under nitrogen for 48 hrs at room temperature. The product was poured into 100 mL of 0.1 M HCl solution to afford a yellowish-brown precipitate. The precipitated product was washed with cold water (four times) and finally with methanol (two times).

The resulting solid was dried in the oven at 50 oC. IR (KBr) v/cm-1: 3442, 3106, 3063, 2229 (C?N), 1598, 1516, 1486, 1244 (C-O-C), 1205, 1076, 840, 727. 1HNMR d-DMSO; ä (ppm): 3.0- 4.0 (m, 10H, CH2); 6.29 (s, 2H, pyrrole), 7.30 (d, 2H, pyrrole); 7.44 (m, 1H, phenyl); 7.85 (d, 1H, phenyl); 8.10(d, 1H, phenyl).

Manganese tetrapentoxy pyrrole phthalocyanine (3, MnTPePyrPc), Scheme 1. The first step was the synthesis of unmetallated tetrapentoxy pyrrole phthalocyanine (10, H2TPePyrPc) by dissolving 1.2 g (4.30 mmol) of 5-(pyrrol-1- yl)pentoxyphthalonitrile (9) in 15 mL dry pentanol and stirring under reflux for 15 minutes. Following this, 10 mg lithium was added to the stirring mixture while stirring and the solution turned green immediately. UV-Visible spectra of the product were used to monitor the formation of the Pc. After 1hr, the product was allowed to cool to room temperature and methanol was added to the solution to precipitate out the product. The product was Soxhlet extracted with methanol for 24 hrs, to remove unreacted phthalonitrile. After this treatment, the product was found to be predominantly metal free Pc. No further purification was done. Complex 10 was used for synthesis of the manganese derivative (3), by reaction of 0.4 g (0.36 mmol) of 10 with 0.027 g (0.023 mmol) of manganese chloride in dry pentanol under reflux for 1 hr. The solution was transferred into distilled methanol to precipitate out the solid 3. Finally, the product was purified by column chromatography using dichloromethane as eluting solvent and its purity was confirmed by thin layer chromatography. Characterization of the products gave satisfactory results.

H2TPePyrPc 10: Yield: 60%. IR (KBr) v/cm-1: 3280, 3097, 2930, 2865, 1615, 1487, 1235 (C-O-C), 1090, 940, 826, 721. UV-Visible (DMF) ëmax/nm (log å) (DMF): 330 (4.48), 635 (4.01), 670 (4.65), 700 (4.65). 1HNMR d-DMSO; ä (ppm): 3.0-4.0 (m, 40H, CH2); 6.19 (d, 8H, pyrolle); 7.32 (d, 8H, pyrrole); 8.41(s, 4H, Pc); 9.00 (s, 8H, Pc).

MnTPePyrPc 3: Yield: 92%. IR (KBr) v/cm-1: 2930, 2856, 2370, 1638, 1509, 1341, 1244 (C-O-C), 1137, 1082, 823. UV-Visible (DMF) ëmax/nm, Log å: 641 (4.4). Anal. Calcd. for C68H68MnN12O4 (1171 gmol-1): C, 69.63%; H, 5.83%; N, 14.29%. Found: C, 68.7%; H, 5.64%; N, 13.56%.

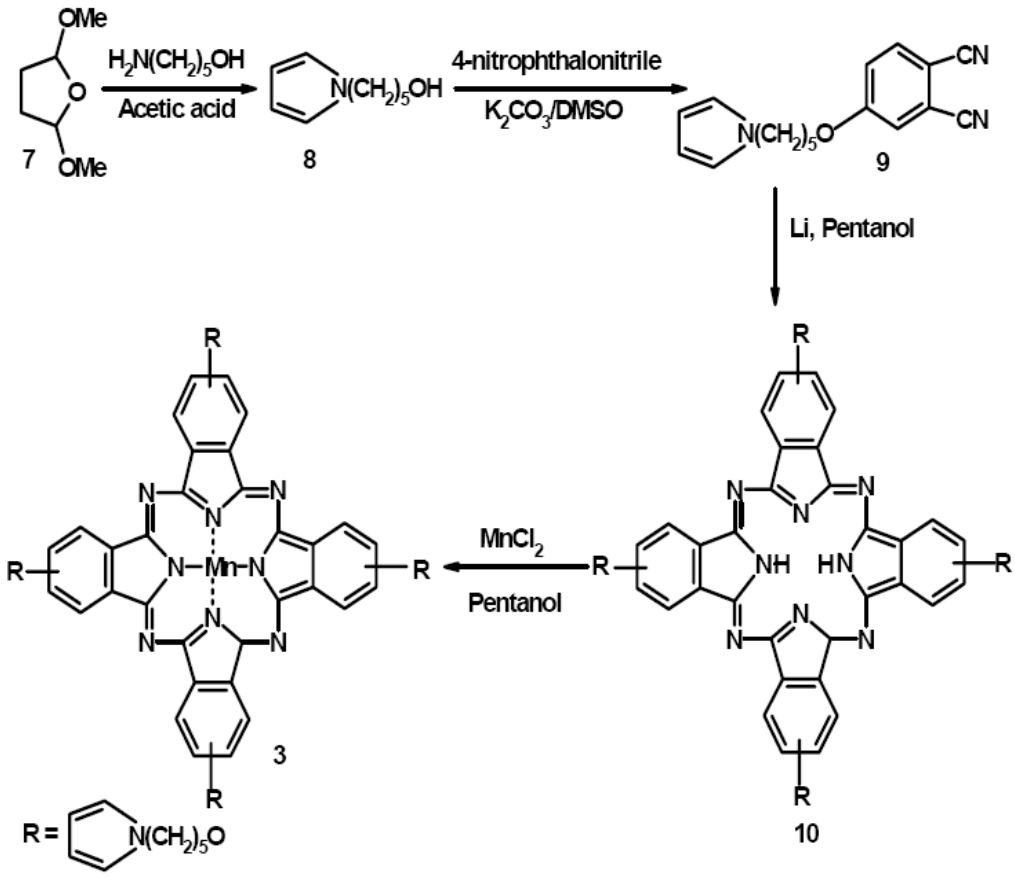

Scheme 1: Synthesis of MnTPePyrPc; complex 3